Longworth, J. W. (1986) in *Time Resolved Fluorescence Spectroscopy in Biochemistry and Biology*, Proceedings of a NATO Advanced Study Institute, St. Andrews (Cundall, R. B., & Dale, R. E., Eds.) pp 651–725, Plenum Press, New York.
Macgregor, R. B., Jr., & Weber, G. (1986) *Nature (London) 318*, 70–73.
Marriott, G., Zechel, K., & Jovin, T. M. (1988) *Biochemistry 27*, 6214–6220.
Meech, S. R., Phillips, D., & Lee, A. G. (1986) *Chem. Phys. 80*, 317–328.
Petrich, J. W., Longworth, J. W., & Fleming, G. R. (1987) *Biochemistry 26*, 2711–2722.
Piston, D., Marriott, G., Clegg, R. M., Radivoyevitch, T., Jovin, T. M., & Gratton, E. (1989) *Rev. Sci. Instrum. 60*, 2596–2600.
Reuben, J. (1979) in *Handbook on the Physics and Chemistry of Rare Earths* (Gschneider, K. A., & Eyring, L., Eds.) pp 515–552, North-Holland Amsterdam.
Richardson, F. (1982) *Chem. Rev. 82*, 541–552.
Richardson, J. S. (1981) *Adv. Protein Chem. 34*, 167–191.
Ross, J. B. A., & Brand, L. (1986) in *Time Resolved Fluorescence Spectroscopy in Biochemistry and Biology*, Proceedings of a NATO Advanced Study Institute, St. Andrews (Cundall, R. B., & Dale, R. E., Eds.) pp 635–643, Plenum Press, New York.
Saris, C. J. M., Tack, B. F., Kristensen, T., Glenney, J. R., & Hunter, T. (1986) *Cell 46*, 201–212.
Scarlata, S., Rholam, R., & Weber, G. (1984) *Biochemistry 23*, 6789–6792.
Shadle, P., Gerke, V., & Weber, K. (1985) *J. Biol. Chem. 260*, 16354–16360.
Siebrand, W. (1966) *J. Chem. Phys. 44*, 4055–4064.
Strickland, E. H., Horwitz, J., & Billups, C. (1970) *Biochemistry 9*, 4914–4921.
Strickland, E. H., Billups, C., & Kay, E. (1972) *Biochemistry 11*, 3657–3662.
Teale, F. W. J. (1960) *Biochem. J. 76*, 381–388.
Valeur, B., & Weber, G. (1977) *Photochem. Photobiol. 25*, 441–444.
Weber, G. (1960) *Biochem. J. 75*, 335–345.
Weber, G. (1983) in *Time Resolved Fluorescence Spectroscopy in Biochemistry and Biology*, Proceedings of a NATO Advanced Study Institute, St. Andrews (Cundall, R. B., & Dale, R. E., Eds.) pp 1–20, Plenum Press, New York.
Weber, K., Johnsson, N., Plessman, U., Van, P. N., Söling, H. D., Ampe, C., & Vandekerckhove, J. (1987) *EMBO J. 6*, 1599–1604.
Willis, K. J., & Szabo, A. G. (1989) *Biochemistry 28*, 4902–4908.
Xu, G.-J., & Weber, G. (1982) *Proc. Natl. Acad. Sci. U.S.A. 79*, 5268–5271.

Folding and Stability of *trp* Aporepressor from *Escherichia coli*†

Mitchell S. Gittelman‡ and C. Robert Matthews*
Department of Chemistry, The Pennsylvania State University, University Park, Pennsylvania 16802
Received November 30, 1989; Revised Manuscript Received April 4, 1990

ABSTRACT: Equilibrium and kinetic studies of the urea-induced unfolding of *trp* aporepressor from *Escherichia coli* were performed to probe the folding mechanism of this intertwined, dimeric protein. The equilibrium unfolding transitions at pH 7.6 and 25 °C monitored by difference absorbance, fluorescence, and circular dichroism spectroscopy are coincident within experimental error. All three transitions are well described by a two-state model involving the native dimer and the unfolded monomer; the free energy of folding in the absence of denaturant and under standard-state conditions is estimated to be 23.3 ± 0.9 kcal/mol of dimer. The midpoint of the equilibrium unfolding transition increases with increasing protein concentration in the manner expected from the law of mass action for the two-state model. We find no evidence for stable folding intermediates. Kinetic studies reveal that unfolding is governed by a single first-order reaction whose relaxation time decreases exponentially with increasing urea concentration and also decreases with increasing protein concentration in the transition zone. Refolding involves at least three phases that depend on both the protein concentration and the final urea concentration in a complex manner. The relaxation time of the slowest of these refolding phases is identical with that for the single phase in unfolding in the transition zone, consistent with the results expected for a reaction that is kinetically reversible. The two faster refolding phases are presumed to arise from slow isomerization reactions in the unfolded form and reflect parallel folding channels.

The great majority of the studies on protein folding have focused on small monomeric globular proteins [for reviews, see Goldenberg (1988), Jaenicke (1987), Creighton (1984), and Kim and Baldwin (1982)]. The high degree of reversibility and the unimolecular folding kinetics have made this class of proteins an attractive target. Although these efforts have the potential to provide information on how the amino acid sequence determines the secondary and tertiary structure, issues on quaternary structure cannot be addressed.

To answer such questions, Jaenicke and others have examined the folding mechanism of a number of dimeric and tetrameric enzymes [see Jaenicke (1987) for a review]. For

†This work was supported by the National Institute of General Medical Sciences, Grant GM23303, and the National Science Foundation, Grant DMB-8705673.
‡Present address: Department of Molecular Biophysics and Biochemistry, Yale University, New Haven, CT 06510.

0006-2960/90/0429-7011$02.50/0

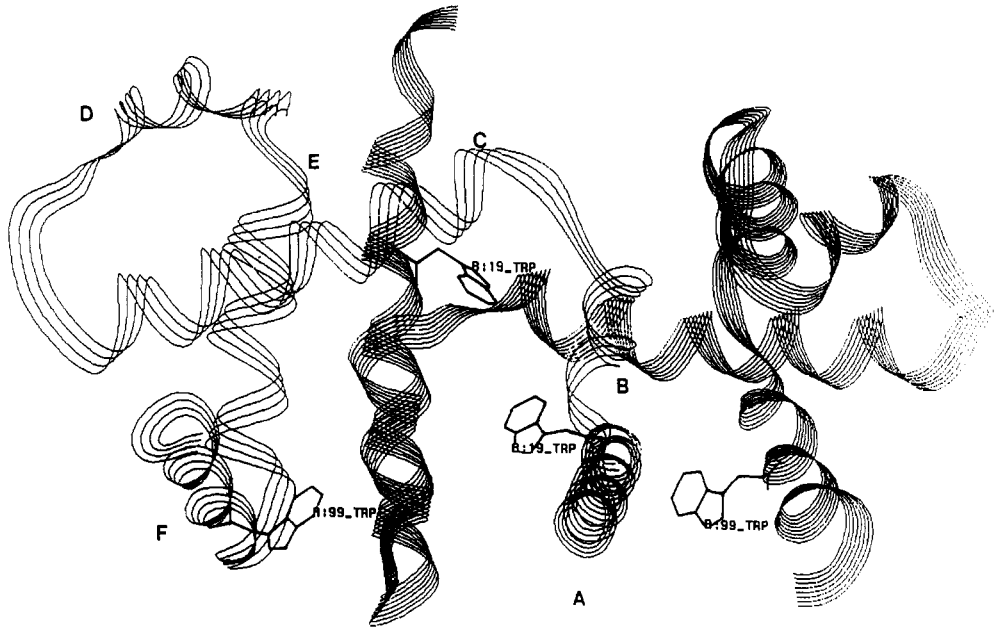

FIGURE 1: Ribbon diagram of *trp* aporepressor (Zhang et al., 1987). The Trp 19 and 99 side chains are displayed and labeled.

example, Jaenicke and Rudolph (1983) proposed that the refolding of lactate dehydrogenase follows a sequential unimolecular/bimolecular pathway containing inactive or partially active monomers. Blond and Goldberg (1986) have identified monomeric and dimeric intermediates along the folding pathway of the dimeric β_2 subunit of tryptophan synthase; the kinetic folding model proposed to explain the results includes seven species. Garel and his colleagues (Vaucheret et al., 1987) have studied the refolding of the dimeric, multidomain aspartokinase-homoserine dehydrogenase and observed significant folding of monomers prior to association. They have also been successful in elucidating the folding mechanism of phosphofructokinase, a tetrameric enzyme that appears to proceed through folded monomers and dimers (Le Bras et al., 1989). Although these studies have provided general kinetic schemes for the folding of oligomeric proteins, the rather large size of the monomers in these enzymes, problems with reversibility (Jaenicke, 1987), and the kinetic complexities involved in the folding of multidomain proteins all suggest that for a detailed study of the important molecular events a simpler system would be advantageous.

The *trp* aporepressor from *Escherichia coli* is a dimeric protein composed of two identical monomers of 107 amino acids (Gunsalus & Yanofsky, 1980); the monomer molecular weight is 12356 (Joachimiak et al., 1983). It is an all α-helical protein containing six helices in each monomer, as seen in the 1.8-Å resolution X-ray structure (Figure 1) (Zhang et al., 1987). Four of the helices from each monomer (A, B, C, and F) are intertwined to form the central core of the dimer; the remaining pair of helices in each monomer, E and F, border this core region and form the DNA reading heads. The biological function of *trp* aporepressor, when complexed with its corepressor, L-tryptophan, is to regulate transcription initiation of three unlinked operons, *aroH* (Zurawski et al., 1981), *trp EDCBA* (Rose et al., 1973), and *trpR* (Gunsalus & Yanofsky, 1980).

Our interest in examining the folding mechanism of *trp* aporepressor was stimulated by the equilibrium unfolding studies conducted by Lane and Jardetzky (1987). Using urea as a denaturant, Lane and Jardetzky reported that unfolding can be studied at concentrations sufficient for NMR spectroscopy. They concluded that unfolding proceeds via a stable intermediate that can be detected by optical and proton magnetic resonance spectroscopies. These results prompted an investigation of the folding kinetics in our laboratory to determine the mechanism of folding and the role of this equilibrium intermediate.

In this paper we report the results of both equilibrium and kinetic studies of the urea-induced unfolding of wild-type *trp* aporepressor. In contradiction to the observations of Lane and Jardetzky (1987), the equilibrium unfolding reaction appears to follow a two-state model involving only the native dimer and the unfolded monomer. Kinetic studies show, however, that additional, transient species are involved in the folding mechanism.

Experimental Procedures

Protein Source and Purification. Wild-type *trp* aporepressor was obtained from *Escherichia coli* strain CY15070 containing the plasmid pJPR2 (a gift from C. Yanofsky) and purified according to the methods reported previously (Paluh & Yanofsky, 1987).

Protein Purity. The purity of the protein was verified by the presence of a single band on Coomassie blue stained $NaDodSO_4$–polyacrylamide gels.[1] Specific activity of *trp* aporepressor was determined to be approximately 4×10^5 units mg^{-1} by the restriction site protection assay described previously (Joachimiak et al., 1983). Additionally, using a gel retardation assay, it was found to have a binding affinity to operator DNA that is comparable to that of samples purified in other laboratories (Carey, 1988).

Reagents and Experimental Conditions. Ultrapure urea was purchased from Schwarz/Mann and used without further purification. All other chemicals were reagent grade. The buffer used in all folding experiments was 10 mM sodium phosphate and 0.1 mM Na_2EDTA, pH 7.6. The temperature was maintained at 25 °C for all experiments unless specified otherwise. Protein concentration was measured by the absorbance at 280 nm and calculated from Beers Law using the extinction coefficient of 2.97×10^4 M^{-1} cm^{-1} (Joachimiak et al., 1983). All aporepressor concentrations are reported for

[1] Abbreviations: $NaDodSO_4$, sodium dodecyl sulfate; Na_2EDTA, ethylenediaminetetraacetic acid disodium salt; CD, circular dichroism.

the dimer unless otherwise specified. Purified protein was stored as a precipitate in 70% ammonium sulfate at 4 °C. Samples were prepared for study by dialysis against the folding buffer and centrifugation at 15600*g* for 10 min to remove any undissolved material.

Spectroscopic Methods. The solution conformation of *trp* aporepressor was examined by three spectroscopic methods: (1) difference ultraviolet (UV) absorbance spectroscopy on an Aviv/Cary 118DS spectrophotometer using the tandem cell technique (Herskovitz, 1967); (2) fluorescence spectroscopy on a Perkin-Elmer MPF-66 spectrofluorimeter (tryptophan fluorescence was induced by exciting the sample at 290 nm and the emission intensity recorded at 349 nm; the band-pass for excitation and emission was 5.0 nm); (3) circular dichroism (CD) spectroscopy at 222 nm using a Jasco J-20 spectropolarimeter. Equilibrium measurements were made after all changes in the spectroscopic property were complete.

The changes in the optical properties of the protein were compared by normalizing each transition curve to the apparent fraction of the unfolded form, F_{app}:

$$F_{app} = (Y_{obs} - Y_{nat})/(Y_{unf} - Y_{nat}) \quad (1)$$

where Y_{obs} is the observed extinction coefficient, fluorescence intensity, or molar ellipticity at a given urea concentration and Y_{nat} and Y_{unf} are the observed values for the native and unfolded forms, respectively, at the same denaturant concentration. A linear dependence of Y_{obs} on the denaturant concentration was observed in both the native and unfolded base-line regions for all spectroscopic methods. Linear extrapolations from these base lines were made to obtain estimates of Y_{nat} and Y_{unf} in the transition region.

Thermodynamic parameters were extracted from the dependence of F_{app} on the urea concentration. This was done by assuming that the unfolding reaction follows a two-state model

$$D \rightleftharpoons^{K} 2U$$

where D is the native dimer, U is the unfolded monomer, and $K = [U]^2/[D]$. It can be shown that

$$F_{app} = ((K^2 + 8K[P_{tot}])^{1/2} - K)/4[P_{tot}] \quad (2)$$

where $[P_{tot}] = 2[D] + [U]$ and corresponds to the total protein concentration in terms of monomer. Given that $K = \exp(-\Delta G/RT)$ and assuming that $\Delta G = \Delta G^{H_2O} + A[\text{urea}]$ (Pace, 1986), the dependence of F_{app} upon the urea concentration can be obtained by fitting the data with a nonlinear least-squares program NLIN (SAS Institute, Cary, NC, 1985). ΔG is the free energy difference between D and U at a given urea concentration and at standard state (1 M in D and U), ΔG^{H_2O} is the value in the absence of denaturant, and A is a fitting parameter that reflects the cooperativity of the unfolding transition.

Kinetic data for slow folding reactions (relaxation times greater than 10–15 s) were obtained by difference absorbance spectroscopy using a manual mixing technique. Changes in absorbance were monitored as a function of time at 292 nm following changes in the denaturant concentration. Folding kinetics on the millisecond time scale were monitored by fluorescence spectroscopy using a Durrum Model D-110 stopped-flow instrument (mixing time 10 ms). Samples were excited at 290 nm with a 5-mm slit width and emission above 325 nm was detected with a Corning C. S. 0–54 ground-glass filter. The stopped-flow spectrophotometer was interfaced to an AT&T PC6300 computer to facilitate data collection with the Asyst software package (Asyst Software Technologies, Inc.). Data fitting was performed by using a nonlinear least-squares program NLIN (SAS Institute, Cary, NC, 1985).

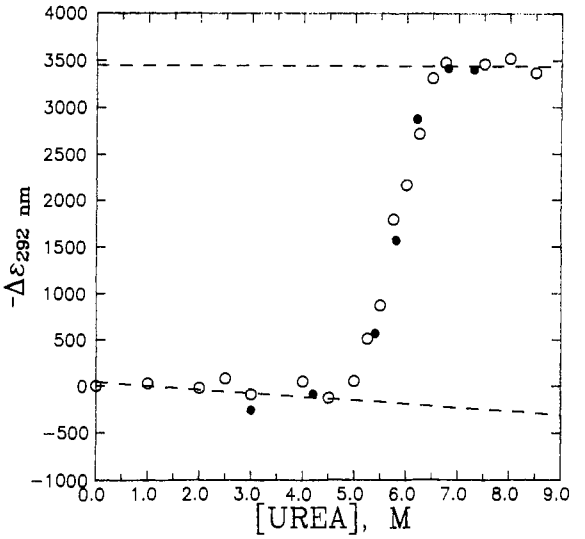

FIGURE 2: Dependence of the extinction coefficient at 292 nm on the urea concentration at pH 7.6 and 25 °C. Samples were unfolded (○) from 0 M urea and refolded (●) from 8.5 M urea. Protein concentration was 14.6 μM. The dashed lines indicate the assumed optical behavior of the native and unfolded protein in the transition region.

The urea dependences of unfolding, k_u, and refolding, k_r, rate constants were fit to the following equations, which are based on transition state theory:

$$k_u = (k_B T/h) \exp(-(\Delta G_u^{*H_2O} - \Delta A_u^{*}[\text{urea}])/RT) \quad (3a)$$

and

$$k_r = (k_B T/h) \exp(-(\Delta G_r^{*H_2O} + \Delta A_r^{*}[\text{urea}])/RT) \quad (3b)$$

where k_B is the Boltzmann constant, h is the Planck constant, R is the gas constant, and T is the absolute temperature. $\Delta G_u^{*H_2O}$ and $\Delta G_r^{*H_2O}$ are the unfolding and refolding activation free energies in the absence of urea and A_u^{*} and A_r^{*} are parameters that account for the observed dependence of the rate constants on denaturant concentration. This approach has been described previously (Matthews, 1987) and has been adapted and extended by others (Kuwajima et al., 1989; Chen & Schellman, 1989).

Solvent accessibilities were calculated from the X-ray coordinates (Zhang et al., 1987) by using the Molecular Surface Program by Connolly (1981). The figure of *trp* aporepressor was generated with a Silicon Graphics Computer System using the program Quanta (v.2).

Results

Equilibrium Studies. The change in extinction coefficient at 292 nm for *trp* aporepressor as a function of urea concentration is presented in Figure 2. The small linear increase in $\Delta\epsilon_{292}$ up to 4.5 M urea reflects the change in solvent composition (Yanari & Bovey, 1960) and indicates that the native protein is stable in this range. The sigmoidal decrease in $\Delta\epsilon_{292}$ from 4.5 to 6.5 M urea represents the cooperative unfolding transition. Above 6.5 M urea the very slight dependence of the extinction coefficient on the urea concentration shows that no further changes in structure occur near the tryptophan residues, which give rise to this signal; the protein is presumed to be unfolded in this range. From a linear extrapolation of the native and unfolded base lines to 0 M urea, we find that the total change in extinction coefficient in the absence of denaturant is $-3400\ M^{-1}\ cm^{-1}$. Using a value of $-1600\ M^{-1}\ cm^{-1}$ for the exposure of a buried tryptophan side chain to

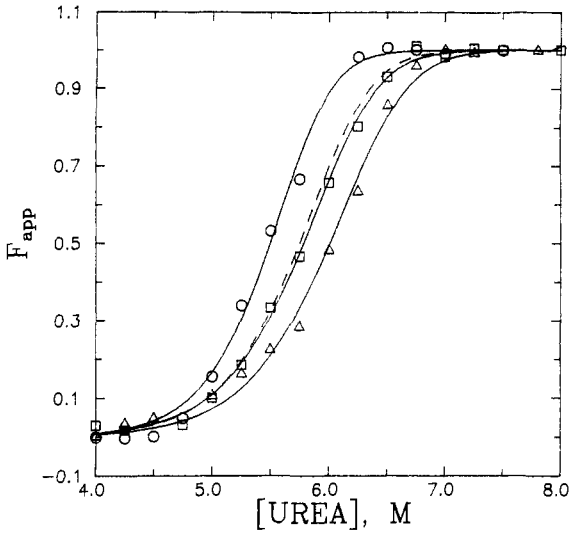

FIGURE 3: Dependence of the apparent fraction of unfolded protein, F_{app}, on the urea concentration at pH 7.6 and 25 °C. The changes in the absorbance at 292 nm were the original data source. Given an error of ± 0.005 au in these measurements, the error in F_{app} is estimated to be ±0.03. Protein concentration was 5.3 μM (○), 19.4 μM (□), and 47.8 μM (△). Lines correspond to fits of the data to eq 2, as described in the Experimental Procedures section. The free energies of unfolding in the absence of denaturant and at standard-state conditions and the midpoints of the transitions obtained from these fits are shown in Table I. The dashed line is the equilibrium unfolding transition curve predicted from the two-state kinetic analysis, eq 8.

solvent upon unfolding (Donovan, 1973), we calculate that unfolding leads to the exposure of 2.1 tryptophan residues per dimer.

The reversibility of this reaction was tested by successively diluting the protein unfolded in 8.5 M urea to lower final urea concentrations and comparing the difference spectrum to that obtained from the unfolding curve (Figure 2). The good agreement between the difference spectra shows that the reaction is more than 95% reversible when unfolded by urea. Reversibility of function was also tested by the restriction site protection assay (Joachimiak et al., 1983); over 90% of the DNA binding capability was recovered following urea denaturation (data not shown).

As a consequence of the dimeric structure of native *trp* aporepressor and the monomeric unfolded form, the apparent stability should depend upon the protein concentration. In Figure 3, it can be seen that as the protein concentration is increased, the midpoint of the difference absorbance unfolding transition is shifted to higher denaturant concentration. At 5.3, 19.4, and 47.8 μM protein, the midpoints of the unfolding transitions are near 5.5, 5.8, and 6.0 M urea, respectively. This trend is consistent with the expectations of the law of mass action and a quantitative fit of this and other data to a two-state model confirms this observation (see below).

Assuming that only the native dimer, D, and unfolded monomer, M, are highly populated during unfolding, these data were fit to a two-state model as described in the Experimental Procedures section. The good agreement between the observed and predicted transition curves at a series of protein concentrations supports the choice of the two-state model (Figure 3). Further support for the validity of this model is provided by the consistent value for ΔG^{H_2O}, 23.2 ± 1.6 kcal mol^{-1}, obtained over an 11-fold range in protein concentration (Table I).

Data collected by fluorescence and CD spectroscopies resulted in unfolding curves similar to that for difference absorbance spectroscopy; no inflections were observed (Figure 4). The fluorescence intensity at 349 nm increased with unfolding (Figure 4A), while the molar ellipticity at 222 nm decreased (Figure 4B). These data (at the same protein concentration) were compared to that from difference absorbance spectroscopy by normalizing the results to the apparent fraction of unfolded protein, F_{app} (Figure 5). The transition curves are coincident within experimental error and all have midpoints near 5.5 M urea. The slightly higher

Table I: Dependence of Free Energy of Unfolding on Protein Concentration[a]

[P][b] (μM)	ΔG^{H_2O} (kcal mol^{-1})	C_m[c] (M)
5.3	24.5 ± 2.2	5.47
14.6	23.3 ± 2.3	5.79
19.4	21.5 ± 1.7	5.76
23.1	24.7 ± 2.1	5.81
33.6	25.4 ± 2.5	5.93
47.8	20.8 ± 1.5	5.98
59.1	22.5 ± 1.6	6.53
	av 23.2 ± 1.6	

[a] Buffers used in all experiments were 10 mM $NaPO_4$, 0.1 mM Na_2EDTA, 25 °C, pH 7.6. Ultraviolet difference absorbance spectra were measured at 292 nm. [b] Protein concentration is in terms of dimer. [c] Urea concentration at the midpoint of the unfolding transition (F_{app} = 0.50) from F_{app} versus [urea] plot (data not shown). Errors in midpoints are ±0.04 M.

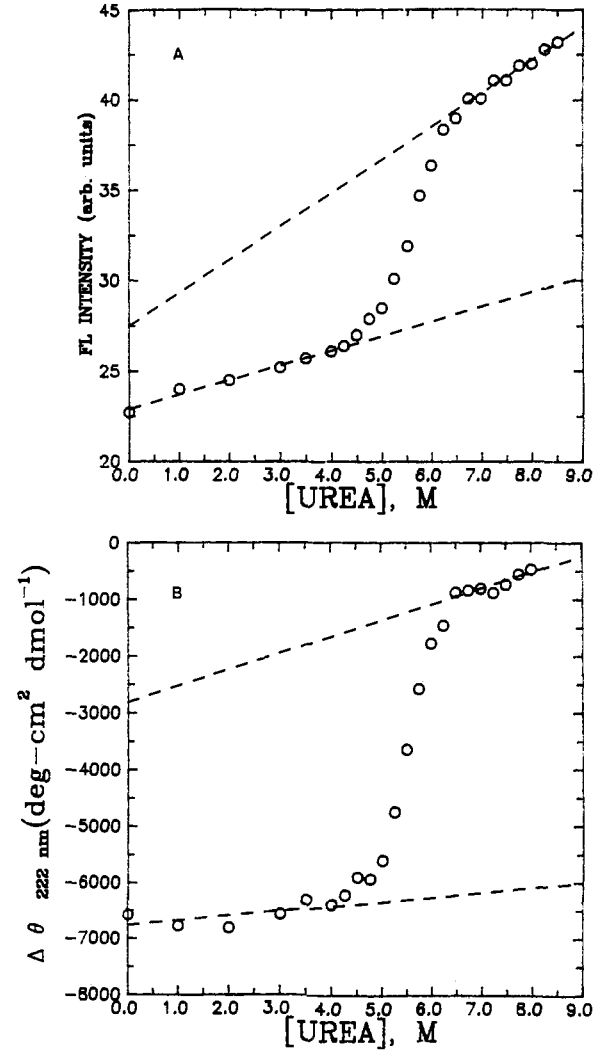

FIGURE 4: Dependence of (A) the fluorescence intensity above 325 nm and (B) the molar ellipticity at 222 nm on the urea concentration at pH 7.6 and 25 °C. The aporepressor concentration was 5.3 μM in both experiments. The dashed lines indicate the assumed optical behavior of the native and unfolded protein in the transition region.

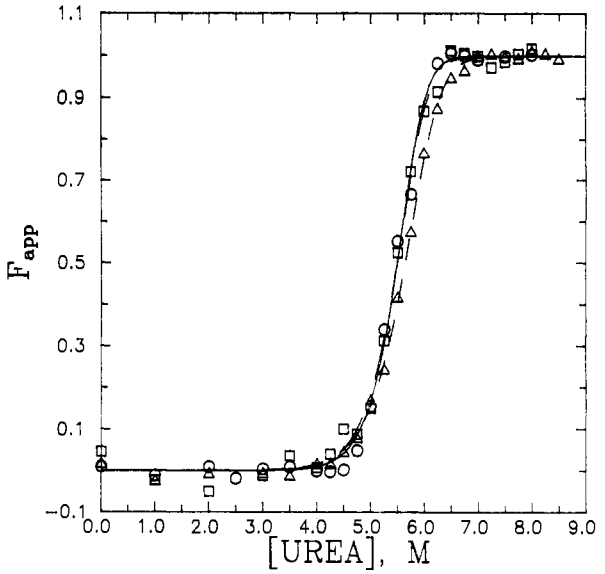

FIGURE 5: Dependence of the apparent fraction of unfolded protein, F_{app}, on the urea concentration at pH 7.6 and 25 °C as monitored by difference absorbance (○), CD (□), and fluorescence (△) spectroscopy. Protein concentration was 5.3 μM in all three experiments.

midpoint for the fluorescence curve probably reflects a steeper unfolded base line for the fluorescence data (Figure 4A), which may introduce a greater systematic error in the equilibrium curve. Fitting these data to the above two-state model, we find that the free energy difference at the standard state is 24.5 ± 2.2, 22.4 ± 1.3, and 23.1 ± 1.7 kcal mol^{-1}, for difference absorbance, fluorescence, and CD spectroscopies, respectively. The excellent agreement between methods that probe the disruption of secondary and tertiary structure also supports a two-state equilibrium model.

Kinetic Studies. The results of the equilibrium experiments are consistent with a two-state folding mechanism for *trp* aporepressor. However, the absence of stable folding intermediates does not preclude the possibility of transient species that could play a critical role in folding. Therefore, the time dependence of absorbance and fluorescence properties were monitored for the unfolding and refolding reactions.

Analysis

The collection and analysis of the kinetic data are complicated both by the dimerization step in refolding and by the requirement to consider both unfolding and refolding rate constants for measurements in and near the transition zone. As a first step in choosing the proper equations with which to fit the data, a series of unfolding/refolding jumps to various final urea concentrations were done at two different protein concentrations. The purpose of these initial experiments was to determine the kinetic order of the unfolding/refolding reactions. For unfolding jumps that ended between 5.25 and 7.0 M urea, the half-life of the absorbance change decreased at higher protein concentration. At 7.0 M urea the half-life became independent of the protein concentration (data not shown). A similar screening of the kinetic order of the refolding reaction showed that the half-life of the refolding reaction decreased at higher protein concentration in the range from 3.5 to 5.0 M urea but became independent of the protein concentration at and below 3.0 M urea (Table II). It should be noted that refolding data below 1.5 M urea could not be collected due to precipitation. Thus, the second-order association/dissociation reaction plays a critical role in determining the kinetic behavior of folding, at least in the region between 3.5 and 7.0 M urea.

Table II: Dependence of the Half-Life for Refolding on the Concentration of *trp* Aporepressor[a]

[urea] (M)	[P][b] (μM)	half-life (s)
2.0	3.0	3.0 ± 0.5
	20.0	2.6 ± 0.4
2.5	3.0	2.9 ± 1.1
	20.0	3.1 ± 0.6
3.0	3.0	3.2 ± 0.8
	20.0	2.9 ± 0.5
3.5	3.0	7.3 ± 1.5
	20.0	3.2 ± 1.3
4.0	3.0	9.3 ± 0.6
	20.0	3.8 ± 1.0
4.5	3.0	40.0 ± 3.5
	20.0	21.7 ± 4.5
5.0	3.0	45.8 ± 3.5
	20.0	21.3 ± 4.0

[a] Half-lives were determined by stopped-flow fluorescence spectroscopy. [b] Protein concentration is in terms of dimer.

Given that the equilibrium data are well described by a simple two-state model, we explored its application to the kinetic data:

$$D \underset{k_r}{\overset{k_u}{\rightleftharpoons}} 2U$$

where k_u is the first-order unfolding rate constant and k_r is the second-order refolding rate constant. For data collected in the range from 3.5 to 7.0 M urea where both unfolding and refolding rate constants can play a significant role in determining the observed relaxation time, we employed the exact expression derived from a relaxation analysis of this system (Bernasconi, 1976):

$$\Delta C(t) = \Delta C(0)(\exp(-t/\tau))/(1 + q\Delta C(0)(1 - \exp(-t/\tau))) \quad (4)$$

where $\Delta C(t)$ is the difference in the concentration of the monomer at time t and at infinite time (when the new equilibrium is achieved), $\Delta C(0)$ is the difference in the concentration of monomer at time zero and at infinite time, τ is the associated relaxation time for the attainment of the new equilibrium, and $q = 4k_r\tau$. If the relaxation process is being monitored by a technique whose signal is linearly proportional to the concentration, e.g., absorbance or fluorescence spectroscopy, it can be shown that the signal change will have the following time dependence:

$$\Delta A(t) = \Delta A(0)(\exp(-t/\tau))/(1 + q'\Delta A(0)(1 - \exp(-t/\tau))) \quad (5)$$

where, for example, $\Delta A(t)$ and $\Delta A(0)$ describe the absorbance properties of the reaction and $q' = q/(\ell(\epsilon_U - \epsilon_{D/2})$. ϵ_U and ϵ_D represent the molar extinction coefficients of the native dimer and unfolded monomer, respectively, and ℓ is the path length in centimeters. For fluorescence measurements, q' would be defined as q divided by terms that relate fluorescence intensity change, ΔF, to the change in protein concentration, ΔC (Cantor & Schimmel, 1980). These terms include the quantum yields of the native dimer and unfolded monomer, the extinction coefficient of the absorbing species, and several instrumental parameters. In our studies, we simply considered q' as a fitting parameter. Note that $q'\Delta F(0) = q\Delta C(0)$.

For unfolding data collected at 7.0 M urea and refolding data at and below 3.0 M urea, where first-order kinetics were observed, the results were fit to a simple exponential or a sum of such terms:

$$A(t) = A(0)\exp(-t/\tau) + A_\infty \quad (6)$$

The parameters are defined as above, with the exception that

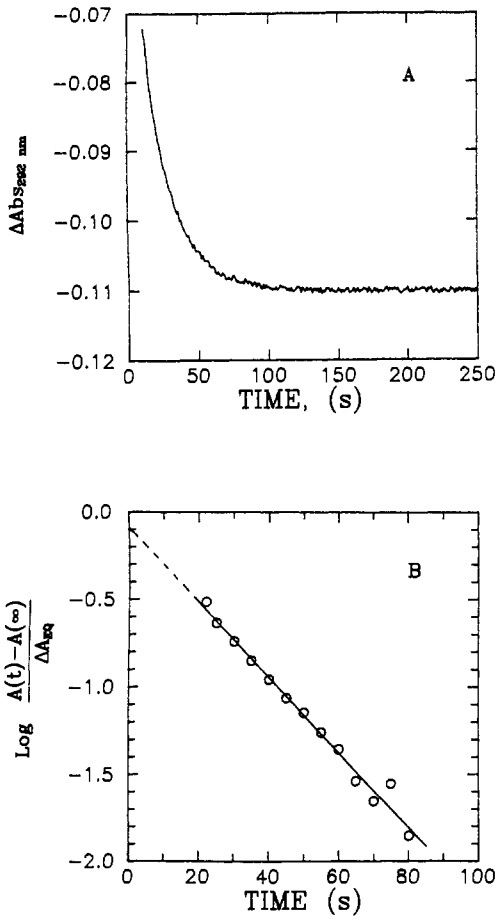

FIGURE 6: (A) Time-dependent change in absorbance at 292 nm from unfolding *trp* aporepressor in 7.0 M urea at pH 7.6 and 25 °C. The protein concentration was 19.4 μM and the initial urea concentration was 0.0 M. (B) Semilog plot of the change in absorbance at 292 nm normalized to the value expected from equilibrium measurements as a function of time. The fit to a single exponential was done with several hundred data points in the time range from 25 to 80 s and is indicated by the solid line; a few representative data points are indicated by the open circles. The dashed line is an extrapolation to the earlier time region.

A_∞ is the amplitude at infinite time.

Unfolding Kinetics

Attempts to fit the unfolding data collected in the transition zone to eq 5 by using a nonlinear least-square fitting program were not consistently successful. After trying and also failing to fit consistently the data to a sum of two and three such terms, the decay curves were trimmed by eliminating the data up to the first half-life and fitting the remainder to a simple exponential (eq 6). The justification for this approach is as follows. For the general system

$$X + X \underset{k_{-1}}{\overset{k_1}{\rightleftharpoons}} X_2$$

the differential equation describing its relaxation behavior is (Bernasconi, 1976)

$$d(\Delta[X])/dt = -(\Delta[X])/\tau - 4k_1(\Delta[X])^2 \qquad (7)$$

The time dependence of $\Delta[X]$ can be reduced to a simple exponential, i.e., the second-order term can effectively be eliminated, in one of two ways: (1) Make the perturbation sufficiently small that $4k_1(\Delta[X])^2 \ll (\Delta[X])/\tau$. (2) Only fit the data corresponding to the latter part of the decay curve. The first approach is not feasible for studying the folding of the *trp* aporepressor because it would require such a small change in the position of the equilibrium so as to make its detection very difficult. The second approach is technically feasible and is valid because the second-order term diminishes more rapidly in the early stages of the reaction than the first-order term; the data can approach simple exponential behavior in the later stages of any complex process (Bernasconi, 1976).

Table III: Urea Dependence of the Relaxation Time and Amplitude for Unfolding of *trp* Aporepressor[a]

[urea] (M)	relax. time (s)	amp ($-\Delta\epsilon_{292nm}$, M^{-1} cm^{-1})	
		kinetics	equilibrium
5.25	27.1	1220	490
5.50	39.3	1350	1110
5.75	41.6	1740	1660
6.00	43.9	2320	2480
6.25	47.0	2980	3130
6.50	47.4	4160	3700
6.75	29.5	3840	4080
7.00	22.4	3490	3980

[a] Protein concentration was 19.4 μM.

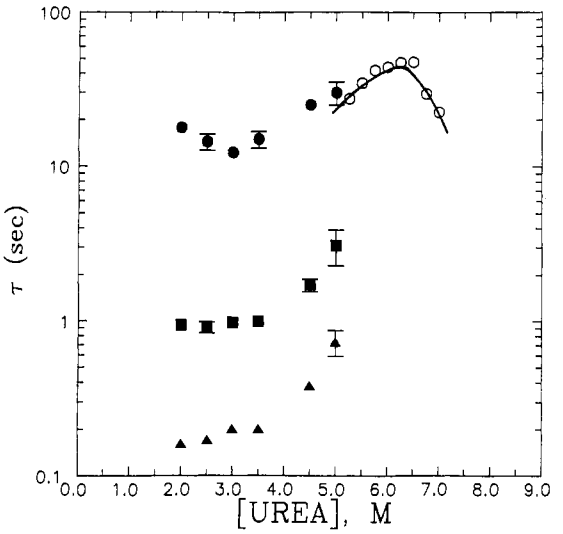

FIGURE 7: Urea dependence of the unfolding (open symbols) and refolding (closed symbols) relaxation times for the τ_1 (○, ●), τ_2 (■), and τ_3 (▲) reactions at pH 7.6 and 25 °C. Protein concentration was 19.4 μM. The unfolding reaction was monitored by difference absorbance at 292 nm and the refolding reaction by stopped-flow fluorescence spectroscopy. The solid line shows the fit of the τ_1 unfolding relaxation times to eq 8; fitting parameters are given in the text.

A representative example of the data collected at 7.0 M urea is shown in Figure 6A; a semilog plot of the normalized absorbance change at 292 nm can be seen in Figure 6B. A single-exponential phase, designated τ_1, is detected, which has a relaxation time of 22.4 s; the amplitude is very close to that expected from the equilibrium experiment. The amplitudes and relaxation times of this single phase in unfolding at various final urea concentrations are shown in Table III. The anomalously high value for the kinetic amplitude at 5.25 M urea probably reflects the error in measuring the small magnitude of the signal in the beginning stages of the unfolding transition. A semilog plot of the dependence of this relaxation time on the final urea concentration is shown in Figure 7. The unfolding relaxation time exhibits a maximum near 6.0 M urea and decreases monotonically as the urea concentration is either increased or decreased from this point.

The failure to consistently fit the unfolding data to eq 5 probably reflects the near-zero values of q' that were obtained in those instances where convergence was possible. For unfolding of the dimer, $q\Delta C(0)$ has a maximum negative value of −0.5 (Bernasconi, 1976) and approaches zero as the equi-

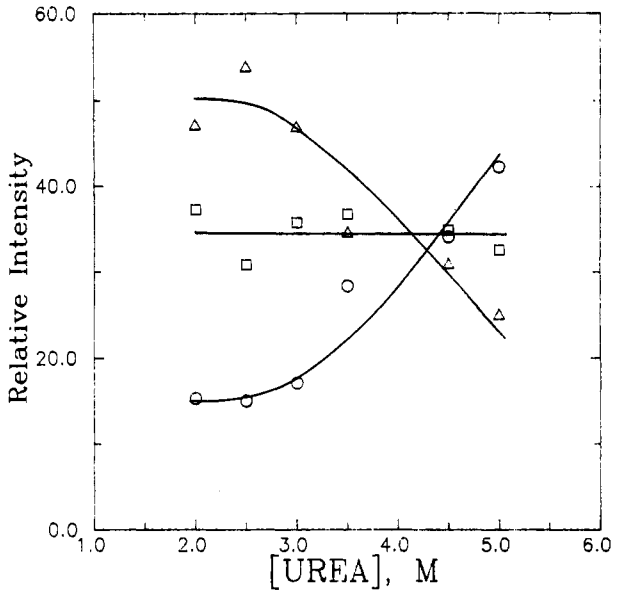

FIGURE 8: Dependence of the amplitudes of the τ_1 (○), τ_2 (□), and τ_3 (△) refolding reactions on the final urea concentration at pH 7.6 and 25 °C as monitored by fluorescence spectroscopy. Protein concentration was 19.4 μM.

librium shifts to favor the unfolded form. As $q\Delta C(0)$ approaches zero, eq 5 becomes equivalent to eq 6. In this case, simple exponential behavior is predicted and observed.

Refolding Kinetics

Attempts to fit the data from refolding jumps ending between 3.5 and 5.0 M urea to eq 5 were unsuccessful. Reasoning that additional phases might be present in refolding [as has been observed in other proteins (Kim & Baldwin, 1982)], we then fit the data to the sum of terms, each of the form shown in eq 5. Three such terms were required to obtain a satisfactory residuals plot (data not shown). The average values of q' for the two faster phases, q'_2 and q'_3, are very close to zero and in fact are negative (−0.03 and −0.11, respectively). The average value of q' for the slowest phase, q'_1, is near unity (1.41) at a variety of final urea concentrations. The negative values for q'_2 and q'_3 are a physical impossibility and probably reflect the optimization of the fit by the program. The first-order refolding data collected between 1.5 and 3.0 M urea also required three terms, each of the form shown in eq 6. The relaxation times and relative amplitudes for each of these phases in refolding at a series of urea concentrations are shown in Figures 7 and 8, respectively.

As can be seen in Figure 7, all three refolding relaxation times decrease monotonically from 5.0 to 3.5 M urea. The τ_1 phase near 5.0 M urea connects smoothly with the single unfolding relaxation time, consistent with an interpretation which proposes that the slowest refolding reaction is the reverse of the unfolding reaction. All three refolding phases connect smoothly with the three first-order reactions that appear at and below 3.0 M urea. The urea and protein concentration independence of the refolding rate constants below 3.0 M urea shows that the nature of the rate-limiting refolding reaction changes under strongly folding conditions. The amplitudes of the τ_1 and τ_3 phases depend upon the final urea concentration, however, the amplitude for the τ_2 phase does not (Figure 8). The loss in amplitude of the τ_3 phase at higher final urea concentrations is compensated by the gain in amplitude of the τ_1 phase; the total change in fluorescence amplitude remains constant.

The activation energy for the unfolding reaction at 7.0 M urea was determined by measuring the rate constant over the temperature range from 15 to 30 °C. The data follow simple Arrhenius behavior with an activation energy of 11.4 ± 3.5 kcal mol^{-1}. The refolding activation energies under strongly folding conditions where first-order behavior is observed (2.0 M urea) were determined over the range from 12 to 27 °C. The activation energies are 25.6 ± 5.7 kcal mol^{-1} for τ_1, 10.1 ± 2.0 kcal mol^{-1} for τ_2, and 10.6 ± 1.0 kcal mol^{-1} for τ_3.

Discussion

Equilibrium Studies. The urea-induced unfolding of the *trp* aporepressor at equilibrium appears to follow a two-state mechanism involving significant populations of only the native dimer and the unfolded monomer. Two lines of evidence support this conclusion:

(1) The unfolding transition curves monitored by difference absorbance, fluorescence, and circular dichroism spectroscopy are coincident within experimental error, at the same protein concentration. Therefore, secondary structure and tertiary structure are disrupted simultaneously.

(2) Each transition curve can be fit to a two-state model, D ↔ 2U. The free energy change under standard-state conditions is independent of the protein concentration or the spectroscopic technique. We find no evidence for stable intermediates in the urea-induced unfolding of *trp* aporepressor.

Calorimetric studies on *trp* aporepressor show that the reversible thermal unfolding process also follows a two-state model (Bae et al., 1988). The free energy difference between the native and unfolded forms at 25 °C can be calculated from this calorimetric data and standard thermodynamic equations (Privalov & Gill, 1988); the value is 15.8 kcal mol^{-1}. This value is significantly less than that obtained from the urea-induced unfolding process and may reflect the observation that the temperature at half-completion of denaturation does not depend significantly on the protein concentration (Bae et al., 1988). It is possible that the thermally unfolded form is a dimer at the protein concentrations required for calorimetry and that only a fraction of the free energy difference is detected.

The two-state behavior reported here contradicts that of a previous study conducted by Lane and Jardetzky (1987), under slightly different conditions (0.1 M $NaPO_4$, pH 7.5, 25 °C). On the basis of the results of optical and NMR experiments, they concluded that a stable intermediate exists in the urea-induced unfolding reaction. We have repeated the fluorescence and circular dichroism experiments using the solution conditions of Lane and Jardetzky and were unable to reproduce their results. In our hands, the results of these experiments also support the two-state model; i.e., we did not observe an inflection in the circular dichroism curve and the fluorescence transition curves obtained by exciting at 290 nm and monitoring the emission at 320 and 370 nm were coincident (data not shown). The reasons for this discrepancy are not apparent; however, differences in sample preparation and/or storage may be significant. As noted above, *trp* aporepressor used in the present study is fully functional in the gel retardation assay developed by Carey (1988).

Kinetic Studies. The data obtained from the *unfolding* kinetic studies are consistent with a simple dynamic equilibrium between the folded dimer (D) and the unfolded monomer (U):

$$D \underset{k_r}{\overset{k_u}{\rightleftharpoons}} 2U$$

To examine the relationship of this reaction to the equilibrium process, the urea dependence of the τ_1 relaxation time

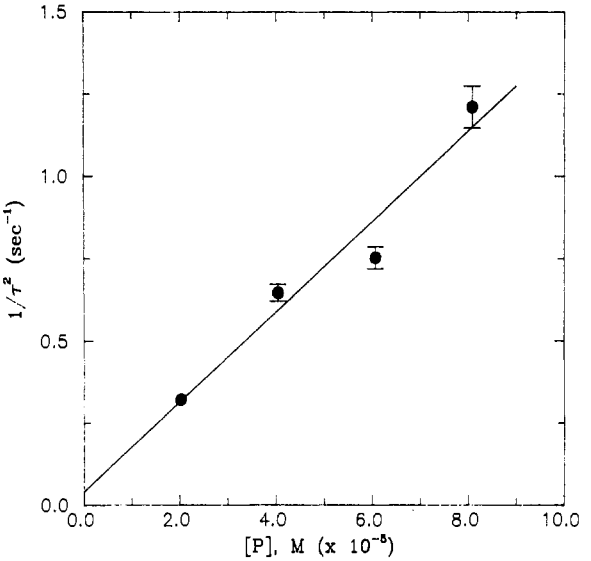

FIGURE 9: Dependence of the relaxation time for unfolding to 5.5 M urea on the protein concentration at pH 7.6 and 25 °C. The initial urea concentration was 0.0 M.

(Figure 7) was used to extract values for the unfolding, k_u, and refolding, k_r, rate constants. The following expression was used to fit the data (Turner et al., 1972):

$$(1/\tau)^2 = 8k_r k_u[P_{tot}] + (k_u)^2 \quad (8)$$

The rate constants, k_u and k_r, were assumed to depend on the urea concentration as shown in the Experimental Procedures section (eqs 3a,b). This procedure yields the following values for the fitting parameters: $\Delta G_u^{*H_2O} = 26.5 \pm 5.3$ kcal mol^{-1}, $A_u^* = 1.0 \pm 0.6$ kcal mol^{-1} M^{-1}, $\Delta G_r^{*H_2O} = 2.3 \pm 3.9$ kcal mol^{-1}, and $A_r^* = 2.0 \pm 0.6$ kcal mol^{-1} M^{-1}. The predicted dependence of τ_1 on the urea concentration using these parameters in eq 8 is shown in Figure 7. The good agreement between the observed and predicted relaxation times supports the choice of the kinetic model. From these parameters the values of k_u and k_r at any urea concentration can be calculated via eqs 3a,b. The equilibrium constant at any urea concentration can then be calculated from $K = k_u/k_r$ and a predicted F_{app} curve at any protein concentration generated from eq 2. The results are shown in Figure 3. The excellent agreement between the unfolding transition curve calculated from the kinetic data and that from equilibrium measurements strongly suggests that the direct unfolding and refolding reaction plays a crucial role in the folding of *trp* aporepressor.

It must be noted that eq 8 is applicable only in the limit of small perturbations, i.e., where the decay curves follow simple exponential behavior. As described above, we approximated this type of behavior by only fitting the data in the latter half of the unfolding decay curves to a simple exponential. The validity of this approach was tested by measuring the dependence of the τ_1 relaxation time for unfolding to 5.5 M urea on the protein concentration. In Figure 9 it can be seen that $(1/\tau_1)^2$ varies linearly with total protein concentration, $[P_{tot}]$, as expected from eq 8. From the slope and intercept of this plot, the values of k_r and k_u at 5.5 M urea can be calculated and are 2.94×10^2 M^{-1} s^{-1} and 5.88×10^{-3} M^{-1} s^{-1}, respectively. These values can be compared to those obtained at 5.5 M urea when eq 8 is used to fit the dependence of the τ_1 relaxation time to the final urea concentration (see above), $k_r = 1.76 \times 10^3$ M^{-1} s^{-1} and $k_u = 3.34 \times 10^{-3}$ M^{-1} s^{-1}. The unfolding rate constants from the two different experiments are within a factor of 2 while the refolding rate constants are within a factor of 6 of each other. This agreement seems reasonably good, considering the approximations required to analyze the data.

The explanation of the refolding data requires a more complex model. Consider first the behavior of the slowest, τ_1, phase. In the transition zone this relaxation time depends on the final urea concentration and is the same as that for the unfolding reaction at the same final urea concentration. At and below 3.0 M urea this relaxation time becomes independent of the urea concentration. This change in urea dependence suggests a change in the nature of the rate-limiting step from folding to isomerization. Two possible models are

model 1

$$D \leftarrow 2U_A \leftarrow 2U_B$$

model 2

$$D \leftarrow D^* \leftarrow 2U$$

In model 1, isomerization occurs in the unfolded monomer between U_B and U_A before association into the dimer. In model 2, isomerization occurs between the dimeric intermediate D* and D, after association. Solely on the basis of the refolding data, either model is satisfactory. When one also considers the unfolding results and the observation that the same urea-dependent reaction is rate-limiting in both directions, model 2 can be eliminated. For model 2 to explain this latter result, one must postulate that D and D* are optically similar (otherwise a second kinetic phase would be detected in unfolding) and that the D $\rightarrow$ D* reaction is always substantially faster than the D* $\rightarrow$ 2U reaction (to allow the second-order refolding reaction to influence τ). Given that D* $\rightarrow$ D is relatively slow (10 s at 25 °C) and assuming that the isomerization reaction is urea independent at all urea concentrations, the equilibrium between D and D* would favor D*. This contradicts the assumption that D* is a folding intermediate.

The postulated isomerization reaction in the unfolded monomers may be due to cis/trans proline isomerization, as has been shown for thioredoxin (Kelley & Richards, 1987) and cytochrome *c* (White et al., 1987) and is strongly suggested for ribonuclease A (Schmid et al., 1986; Schmid & Baldwin, 1978). An activation energy of 25.6 kcal mol^{-1} for the τ_1 phase under strongly refolding conditions (2.0 M urea) where the relaxation time is independent of both urea and protein concentration is consistent with this proposal. Because all four X-Pro peptide bonds in the *trp* aporepressor are in the trans configuration in the native conformation (P. Sigler, personal communication), it is puzzling that only a single kinetic phase is apparent in refolding through this channel. Both U_A and U_B would be expected to be significantly populated and to contribute a fast, urea-dependent phase and a slow, urea-independent phase, respectively, at low urea concentrations. The failure to detect both phases may be due to the inability to collect data at and below 1.5 M urea where the phases would separate and be observable. Alternatively, the U_A species may not be highly populated under unfolding conditions.

The τ_2 and τ_3 refolding phases are similar to the τ_1 phase in that the relaxation times follow the same pattern as a function of urea concentration; however, they differ in the activation energies for refolding to 2.0 M urea. Because these activation energies, 10.1 and 10.6 kcal mol^{-1}, respectively, are substantially less than that expected for proline isomerization, it is possible that these isomerization reactions do occur after association in additional folding channels. Baldwin and his colleagues have shown that ribonuclease A can fold to a nativelike species with an X-Pro peptide bond in the nonnative

isomeric form (Nall et al., 1978). In this case, the activation energy of the isomerization reaction is decreased by 10–15 kcal mol^{-1} by the folded protein.

A mechanism that incorporates all of the kinetic data is as follows:

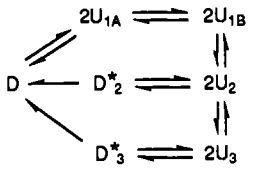

Two additional populations of unfolded monomer, U_2 and U_3, associate with another monomer from the same manifold to form the respective dimer intermediates, D^*_2 and D^*_3, via urea-dependent folding reactions that are rate-limiting between 3.5 and 5.0 M urea. These dimers then isomerize to the native dimer, D, via urea-independent reactions that are rate-limiting only below 3.0 M urea. A possible variation on this scheme is to eliminate the U_3 species and allow the U_2 species to associate with U_{1A} in the third folding channel.

The variation in the amplitudes of the three refolding phases as a function of the final urea concentration (Figure 8) provides insight into the stabilities of the putative dimeric intermediates D^*_2 and D^*_3. While the amplitudes at low urea concentration reflect the distribution of the unfolded species in the above model, the *change* in the amplitudes as the final urea concentration is increased reflects the relative stability of the intermediate dimers. The decrease in the relative amplitude of the τ_3 phase and the corresponding increase in the amplitude of the τ_1 phase suggest that D^*_3 is selectively destabilized at higher urea concentration. This decrease in stability results in a smaller fraction of material flowing through this channel and an increased fraction flowing in the τ_1 channel. Inspection of Figure 8 also suggests that the amplitude of the τ_1 channel exceeds that of the τ_2 channel in the transition region. If the trend shown continues then the majority of the unfolded protein will fold through the τ_1 channel at final urea concentrations that correspond to the equilibrium transition zone. In this case, the kinetic model would simplify to $D \leftrightarrow 2U_A \leftrightarrow 2U_B$ and exhibit a simple two-state equilibrium behavior. The excellent agreement between the equilibrium transition curve and that obtained from the kinetic analysis (Figure 3) supports this proposal.

Similar effects of the final urea concentration on the amplitudes of certain refolding phases have been observed in thioredoxin (Wilson et al., 1986) and in a fragment of a κ immunoglobin light chain (Goto et al., 1988). Both groups attributed the decrease in amplitudes at higher denaturant concentration to the marginal stability of transient intermediates.

We view the above folding model for *trp* aporepressor as a *working* model that serves to evaluate our current data and that can be used to design tests of its validity. For example, as yet we have no direct evidence for a series of unfolded forms that interconvert slowly relative to folding. We simply postulate their existence as a means of accounting for the observation of three protein concentration dependent refolding reactions in the formation of a dimer.

The apparent absence of either transient or stable folding intermediates in the τ_1 folding channel for the *trp* aporepressor is rather surprising. The intertwined nature of the structure (Figure 1) might lead one to expect such species. On the basis of the kinetic data from absorbance and fluorescence spectroscopy, it appears that folding and association are a concerted process. This conclusion must be viewed with some caution because only one tryptophan in each subunit probably gives rise to the bulk of the absorbance and fluorescence changes in folding. Both Trp 19 residues are buried in the core at the interface between the subunits and are only marginally exposed to solvent (9 $Å^2$). The remaining tryptophan, Trp 99, has a greater solvent exposure (34 $Å^2$) and may be less sensitive to the folding process (Figure 1). The magnitude of the change in extinction coefficient at 292 nm upon unfolding is consistent with this proposal as is the differential quenching of tryptophan fluorescence (Lane & Jardetzky, 1987). Although the two Trp 19 residues are very likely to be affected by the subunit association reaction, they may well be insensitive to folding in peripheral regions. Given the high helical content in both the core and DNA reading head regions of *trp* aporepressor, kinetic studies of the ellipticity might provide some clues as to the formation of structure in the monomers prior to or following association.

Acknowledgments

We express our deep appreciation to Dr. Charles Yanofsky for providing bacterial strains of *trp* aporepressor containing the plasmid pJPR2 and to Dr. Juliette Lecomte for a critical review of this manuscript and helpful suggestions. We are also grateful to Dr. Randy Zauhar from the Biocomputing Center of The Pennsylvania State University Biotechnology Institute for calculations of the solvent-accessible surface areas and Aleister Saunders for generating the figure of *trp* aporepressor. We thank Gail Feldman for typing this manuscript.

References

Bae, S.-J., Chou, W.-Y., Matthews, K., & Sturtevant, J. M. (1988) *Proc. Natl. Acad. Sci. U.S.A. 85*, 6731.

Beasty, A. M., Hurle, M. R., Manz, J. T., Stackhouse, T., Onuffer, J. J., & Matthews, C. R. (1986) *Biochemistry 25*, 2965.

Bernasconi, C. F. (1976) *Relaxation Kinetics*, Academic Press, New York.

Blond, S., & Goldberg, M. E. (1986) *Proteins 1*, 247.

Cantor, C. R., & Schimmel, P. R. (1980) *Biophysical Chemistry*, Freeman, New York.

Carey, J. (1988) *Proc. Natl. Acad. Sci. U.S.A. 85*, 975.

Chen, B.-L., & Schellman, J. A. (1989) *Biochemistry 28*, 685.

Connolly, M. L. (1981) *QCPE 1*, 74.

Creighton, T. E. (1984) *Proteins, Structure and Molecular Principles*, W. H. Freeman, New York.

Donovan, J. W. (1973) *Methods Enzymol. 27*, 497.

Goldenberg, D. P. (1988) *Annu. Rev. Biophys. Biophys. Chem. 17*, 481.

Goto, Y., Ichimura, N., & Hamaguchi, K. (1988) *Biochemistry 27*, 1670.

Gunsalus, R. P., & Yanofsky, C. (1980) *Proc. Natl. Acad. Sci. U.S.A. 77*, 7117.

Herskovitz, T. T. (1967) *Methods Enzymol. 11*, 748.

Jaenicke, R. (1987) *Prog. Biophys. Molec. Biol. 49*, 117.

Jaenicke, R., & Rudolph, R. (1983) *Biological Oxidations* (Sund, H., & Ullrich, V., Eds.) Vol. 34, p 62, Colloquium Mosbach, Springer Verlag, Berlin.

Joachimiak, A., Kelley, R. L., Gunsalus, R. P., Yanofsky, C., & Sigler, P. B. (1983) *Proc. Natl. Acad. Sci. U.S.A. 79*, 3120.

Kelley, R. F., & Richards, F. M. (1987) *Biochemistry 26*, 6765.

Kim, P. S., & Baldwin, R. L. (1982) *Annu. Rev. Biochem. 51*, 459.

Kuwajima, K., Mitani, M., & Sugai, S. (1989) *J. Mol. Biol. 206*, 547.

Kuwajima, K., Sakuraoka, A., Shoichi, F., Yoneyama, M., & Sugai, S. (1988) *Biochemistry 27*, 7419.
Lane, A. N., & Jardetzky, O. (1987) *Eur. J. Biochem. 164*, 389.
Le Bras, G., Teschner, W., Deville-Bonne, D., & Garel, J. R. (1989) *Biochemistry 28*, 6836.
Matthews, C. R. (1987) *Methods Enzymol. 154*, 498.
Nall, B. T., Garel, J.-R., & Baldwin, R. L. (1978) *J. Mol. Biol. 118*, 317.
Pace, C. N. (1986) *Methods Enzymol. 131*, 266.
Paluh, J. L., & Yanofsky, C. (1986) *Nucl. Acids Res. 14*, 7851.
Privalov, P. L. & Gill, S. J. (1988) *Adv. Protein Chem. 39*, 191.
Rose, J. K., Squires, C. L., Yanofsky, C., Yang, H. L., & Zubay, G. (1973) *Nature (London) New Biol. 245*, 133.
Schmid, F. X., Grafl, R., Wrba, A., & Beintema, J. J. (1986) *Proc. Natl. Acad. Sci. U.S.A. 83*, 872.
Schmid, F. X., & Baldwin, R. L. (1978) *Proc. Natl. Acad. Sci. U.S.A. 75*, 4764.
Touchette, N. A., Perry, K. M., & Matthews, C. R. (1986) *Biochemistry 25*, 5445.
Turner, D. H., Flynn, G. W., Lundberg, S. K., Faller, L. D., & Sutin, N. (1972) *Nature 239*, 215.
Vaucheret, H., Signon, L., Le Bras, G., & Garel, J. R. (1987) *Biochemistry 26*, 2785.
White, T. B., Berget, P. B., & Nall, B. T. (1987) *Biochemistry 26*, 4358.
Wilson, J., Kelley, R. F., Shalongo, W., Lowery, D., & Stellwagen, E. (1986) *Biochemistry 25*, 7560.
Yanari, S., & Bovey, F. A. (1960) *J. Biol. Chem. 235*, 2818.
Zhang, R.-G., Joachimiak, A., Lawson, C. L., Schevitz, R. W., Otwinowski, Z., & Sigler, P. B. (1987) *Nature 327*, 591.
Zurawski, G., Gunsalus, R. P., Brown, K. D., & Yanofsky, C. (1981) *J. Mol. Biol. 145*, 47.

Structure and Function of Hemoglobin Variants at an Internal Hydrophobic Site: Consequences of Mutations at the β 27 (B9) Position†

Yuê Huang,‡ Josée Pagnier,*,‡ Philippe Magne,‡ Faouzi Baklouti,§ Jean Kister,‡ Jean Delaunay,§ Claude Poyart,‡ Giulio Fermi,∥ and Max F. Perutz∥

Institut National de la Santé et de la Recherche Médicale, Unité 299, Hôpital de Bicêtre, 94275 Le Kremlin-Bicêtre, France, Centre National de la Recherche Scientifique, Unité de Recherche Associée 1171, Faculté de Médecine Grange-Blanche, 69373 Lyon Cedex 08, France, and MRC Laboratory for Molecular Biology, Hills Road, Cambridge CB2 2QH, England

Received January 19, 1990; Revised Manuscript Received April 9, 1990

ABSTRACT: We have studied the structure–function relationships in newly discovered hemoglobin (Hb) mutants with substitutions occurring at the tight and highly hydrophobic cluster between the B and G helices in the β chains, namely, Hb Knossos or β A27S and Hb Grange-Blanche or β A27V. The β A27S mutant has a 50% decrease in oxygen affinity relative to native human Hb A, while the β A27V mutant has an increased oxygen affinity. We have also engineered the artificial β A27T mutation through site-directed mutagenesis. This new mutant exhibits functional properties similar to those of Hb A. None of these mutants is unstable. X-ray analyses show that the substitution of Val for Ala may reduce the relative stability of the T structure of the molecule through packing effects in the β chains; for the β A27S mutant a new hydrogen bond between serine and the carbonyl O at β 23 (B5) Val is observed and is likely to increase the relative stability of the T structure in the mutant hemoglobin. However, no significant changes in the crystals were observed for these mutants between the quaternary R and T structures relative to native Hb A. We conclude that small tertiary structural changes in the tight hydrophobic B–G helix interface are sufficient to induce functional abnormalities resulting in either low or high intrinsic oxygen affinities.

Two hemoglobin (Hb)[1] natural variants have been reported recently at the β 27 (B9) site, namely Hb Knossos (A27S) (Fessas et al., 1982; Baklouti et al., 1986) and Hb Grange-Blanche (A27V) (Baklouti et al., 1987). These mutants are of particular interest as they occur at the tight and highly hydrophobic cluster between the B and G helices in the β chains. X-ray analyses (Baldwin & Chothia, 1979; Shanaan, 1983; Fermi et al., 1984) have shown that in native Hb A this portion of the β chains does not undergo significant structural changes on oxygen binding. Substitution of the polar Ser residue for Ala in Hb Knossos leads to a 50% decrease in oxygen affinity; substitution of the more hydrophobic Val for Ala in Hb Grange-Blanche leads to an increased oxygen affinity. To understand more precisely the reasons for the abnormal oxygen affinities of these natural mutants, we have

† This work was supported by funds from Institut National de la Santé et de la Recherche Médicale, from La Direction des Recherches, Etudes et Techniques, from l'Air Liquide Co., and from La Fondation pour la Recherche Médicale.

* To whom correspondence should be addressed.
‡ INSERM U 299.
§ CNRS URA 1171.
∥ MRC Laboratory for Molecular Biology.

[1] Abbreviations: Hb, hemoglobin; DPG, 2,3-diphosphoglycerate; P_{50}, oxygen partial pressure at half-saturation; n_{50}, Hill coefficient at half-saturation; Bistris, bis(2-hydroxyethyl)aminotris(hydroxymethyl)-methane; HEPES, 4-(2-hydroxyethyl)-1-piperazineethanesulfonic acid.

0006-2960/90/0429-7020$02.50/0